

# Study of low-energy magnetic excitations in single-crystalline $\text{CeIn}_3$ by inelastic neutron scattering

W. Knafo, S. Raymond, B. Fakz, G. Lapertoty, P. C. Canfield and J. Flouquet

CEA-Grenoble, DRFM C/SP SM S/M DN, 38054 Grenoble Cedex, France  
ISIS Facility, Rutherford Appleton Laboratory, Chilton, Didcot, Oxon OX11 0QX, England

AMES Laboratory, Iowa State University, Ames Iowa 50011, USA

Abstract.

Inelastic neutron scattering experiments were performed on single crystals of the heavy-fermion compound  $\text{CeIn}_3$  for temperatures below and above the Neel temperature,  $T_N$ . In the antiferromagnetically ordered phase, well-defined spin-wave excitations with a bandwidth of 2 meV are observed. The spin waves coexist with quasielastic (QE) Kondo-type spin-fluctuations and broadened crystal-field (CF) excitations below  $T_N$ . Above  $T_N$ , only the QE and CF excitations persist, with a weak temperature dependence.

PACS numbers: 71.27.+a, 75.40.Gb, 78.70.Nx

Submitted to: Institute of Physics Publishing

Printed: 14 April 2024

## 1. Introduction

A quantum critical point (QCP) occurs in the heavy fermion (HF) compound  $\text{CeIn}_3$  under a hydrostatic pressure of  $P_C = 25$  kbar. This corresponds to a transition at  $T = 0$  K from a magnetically ordered to a disordered state. It was found that at least up to 23 kbar the ground state is antiferromagnetically ordered with a propagation vector  $\mathbf{k} = (\pi/2; \pi/2; \pi/2)$ . At ambient pressure the Neel temperature is  $T_N = 10.1$  K and the staggered magnetization is  $m_0 = 0.5 \mu_B$  [1, 2].  $\text{CeIn}_3$  becomes superconducting below  $T_C = 200$  mK in the vicinity of  $P_C$  [3, 4]. More generally, the appearance of unconventional superconductivity around  $P_C$  in HF systems is supposed to be related to the enhancement of magnetic fluctuations when  $T_N \rightarrow 0$ .

$\text{CeIn}_3$  crystallizes in the cubic  $\text{AuCu}_3$  structure, and hence the magnetic fluctuations are expected to be three-dimensional (3D). This is confirmed by resistivity measurements, which show a  $\rho = T^{3=2}$  non-Fermi liquid (NFL) behavior at the critical

pressure, as expected for 3D fluctuations in spin-fluctuation theories [5, 6]. Recently, a new family of HF compounds was discovered [7],  $\text{Ce}_m\text{T}_n\text{In}_{3m+2n}$ , which is composed of alternating layers of  $\text{CeIn}_3$  and  $\text{TIn}_2$  stacked along the  $c$ -direction with  $T = \text{Ir, Rh, or Co}$ . Their main interest arises from the layered structure that is thought to induce 2D fluctuations that would enhance the superconductivity more than 3D fluctuations near  $T_C$  [8]. Indeed,  $\text{CeCoIn}_5$  has a superconducting state at ambient pressure below  $T_C = 2.3 \text{ K}$ , the highest  $T_C$  observed up to now in HF systems [9]. These recent results motivated us to reinvestigate the common brick of these quasi 2D compounds: the 3D heavy fermion  $\text{CeIn}_3$ .

Previous inelastic neutron scattering (INS) studies on powder samples of  $\text{CeIn}_3$  [10, 11] showed the existence of a crystal field (CF) excitation at  $\omega_{\text{CF}} \approx 12 \text{ meV}$  with a large broadening ascribed to the Kondo effect. In this work, we present new INS measurements on single crystals, which due to new flux growing methods are now sufficiently large for such studies. These measurements show the existence of well-defined spin-wave excitations in the magnetically ordered phase, which coexist with quasielastic (QE) Kondo-type spin-fluctuations and the previously observed broadened crystal-field excitations.

## 2. Experimental details

The single crystals used in this study were grown by the self flux method [12]. A first set of neutron scattering measurements was carried out on the time-of-flight chopper spectrometer MARI at ISIS, using incident energies of 22 and 60.3 meV. The corresponding energy resolution was approximately 2 and 5 meV, respectively. Because of the strong neutron absorption cross-section of In, the single crystals were cut to a thickness of 2 mm and used in transmission geometry. A total of 30 crystals with total weight of 13 g were aligned and glued to a thin aluminum plate, which was mounted in a closed-cycle refrigerator. The mosaicity of the assembly was approximately 6°. Measurements were performed in the  $(hkl)$  plane, with an angle between the incident wavevector and the  $[001]$  direction of 2.5 and 30°.

A second set of neutron scattering measurements was made on the triple-axis spectrometer IN22 at the ILL (Grenoble, France). Pyrolytic graphite was used for the vertically focusing monochromator and the horizontally focusing analyzer. A PG filter in the scattered beam was used to suppress higher order contamination, and final neutron energies of 8.05 and 14.7 meV were used, giving an energy resolution of 0.5 and 1.0 meV, respectively. Two thin plates of the assembly used on MARI were aligned on an aluminum support and mounted in a helium flow "orange" cryostat. The total mass of the sample was about 1 g and the mosaicity 0.5°. The  $(hkl)$  scattering plane was investigated.

## 3. Results

### 3.1. Crystal-field excitation and quasielastic line

For the two crystal orientations used on MARI and at temperatures of  $T = 5, 15$  and  $150$  K, we recorded  $(Q; E)$  intensity maps for  $0 < Q < 10 \text{ \AA}^{-1}$  and  $E < 30 \text{ meV}$ , where  $Q$  is the wavevector transfer and  $E$  is the energy transfer. Despite strong phonon contamination from both the CeIn<sub>3</sub> sample and the Al support, we observed an excitation around  $12 \text{ meV}$  which was independent of the crystal orientation and whose intensity decreased with  $Q$ . The temperature dependence of the  $12 \text{ meV}$  excitation obtained for  $Q < 2 \text{ \AA}^{-1}$  is shown in figure 1. The excitation shows only a very slight softening and broadening as the temperature goes from the ordered state at  $T = 5 \text{ K}$  to the paramagnetic state at  $T = 15 \text{ K}$ . At much higher temperatures,  $T = 150 \text{ K}$ , the excitation is partly suppressed. Figure 2 shows the wavevector dependence of the excitation spectrum at  $T = 5 \text{ K}$ . The peak at  $12 \text{ meV}$  observed at low  $Q$  (integration over  $0 < Q < 2 \text{ \AA}^{-1}$ ) disappears at higher wave vectors (integration over  $7.5 < Q < 7.8 \text{ \AA}^{-1}$ ), reflecting its magnetic nature. The contribution around  $20 \text{ meV}$ , seen only at high  $Q$ 's, is due to phonons. The  $Q$  and  $T$  dependence of the  $12 \text{ meV}$  excitation, as illustrated in Figs. 1 and 2, clearly show its magnetic origin, and corresponds to the CF excitation observed in powder samples by Lawrence et al. [10] and Murani et al. [11].

The cubic environment of  $\text{Ce}^{3+}$  in CeIn<sub>3</sub> can be treated in terms of Stevens operators by the following CF Hamiltonian:  $H_{\text{CF}} = B_4(O_4^0 + 5O_4^4)$  [13]. This Hamiltonian splits the  $J = 5/2$  spin-orbit level of  $\text{Ce}^{3+}$  into a  $\Gamma_8$  quartet and a  $\Gamma_7$  doublet. In the case of CeIn<sub>3</sub>, susceptibility measurements indicates that  $B_4 > 0$  [14], implying that the ground state is  $\Gamma_7$ . This has been confirmed by polarized neutron scattering measurements, which also reveals an admixture of  $\Gamma_8$  to the ground state  $\Gamma_7$  in the ordered phase [15]. The excitation observed here at  $12 \text{ meV}$  corresponds then to the  $\Gamma_7 \rightarrow \Gamma_8$  excitation.

In addition to the  $12 \text{ meV}$  CF excitation, it is clear from the data that there is an additional quasielastic (QE) component to the scattering. The low- $Q$  data at  $T = 5 \text{ K}$  were therefore analyzed using three components: an incoherent elastic peak, a quasielastic spin-fluctuation contribution, and a crystal-field excitation. Since the different contributions partly overlap, we fixed the width (halfwidth at halfmaximum, HWHM)  $\Gamma_{\text{QE}}$  of the QE contribution to  $k_B T_K = 0.86 \text{ meV}$  where  $T_K = 10 \text{ K}$  is the Kondo temperature. The results of the analysis at  $T = 5 \text{ K}$  give a crystal-field splitting of  $\Delta_{\text{CF}} = 10.6 \pm 0.2 \text{ meV}$  and a broadening of the CF levels (HWHM) of  $\Gamma_{\text{CF}} = 5.7 \pm 0.2 \text{ meV}$ . No significant difference in the values of the CF excitations were found for the different orientations of the crystal. At  $T = 15 \text{ K}$ , the resulting CF splitting is  $\Delta_{\text{CF}} = 9.4 \pm 0.2 \text{ meV}$  and its width is  $\Gamma_{\text{CF}} = 6.0 \pm 0.2 \text{ meV}$ . The slight softening observed of  $\Delta_{\text{CF}}$  is related to the splitting of the CF levels below  $T_N$ .

### 3.2. Spin wave

The dispersive mode that appears below  $T_N$  was first observed using the MARI chopper spectrometer. Because of the 3D character of this mode, the study of its dispersion was continued using the IN22 triple-axis spectrometer. Energy scans up to  $6 \text{ meV}$  energy

transfer were measured for different values of the wavevector transfer  $Q$ . Figure 3 shows spectra of CeIn<sub>3</sub> at  $Q = (\frac{1}{2}; \frac{1}{2}; 0.5)$  for  $T = 1.5$  and 15 K. This corresponds to the reduced wavevector  $q = Q - k = (0.3; 0.3; 0)$ , where  $\Gamma = (1; 1; 1)$  is a reciprocal lattice vector and  $k = (\frac{1}{2}; \frac{1}{2}; \frac{1}{2})$  is a magnetic propagation vector (wavevectors are expressed in reciprocal lattice unit with 1 r.l.u. =  $2\pi/a$ , where  $a = 4.689$  Å is the lattice parameter). Figure 3 clearly shows that the excitation present at  $T < T_N$  disappears for  $T > T_N$ . For each wavevector  $q$ , the excitation was fitted by a Gaussian whose width corresponds to the instrumental resolution. The strong dispersion of this excitation in the three main directions of the crystal is shown in figure 4. Since the direction of the ordered moment in CeIn<sub>3</sub> is unknown and our sample is in a multidomain state, it is not possible to determine the polarization of the excitation; it will be assumed to be transverse as for a conventional spin wave.

Supposing that the CF energy is of the same order as the exchange interaction, it seems appropriate to treat the spin wave using the so-called molecular-field random-phase approximation [16]. Writing the exchange Hamiltonian as

$$H_{\text{ex}} = \sum_{i,j} I_{ij} J_i J_j \quad (1)$$

gives the general dispersion relation

$$E(q) = f[M^2 I(q)][M^2 I(q+k)]g^{1/2}; \quad (2)$$

where  $k$  is the propagation vector of the ordered state,  $I(q)$  the Fourier transform of the exchange interaction  $I_{ij}$ , and  $\Gamma$  the splitting of the  $\Gamma$  doublet into  $\Gamma_{7,1}$  and  $\Gamma_{7,2}$  due to the molecular and anisotropy fields. The transition matrix element between the ground state  $\Gamma_{7,1}$  and the first excited state  $\Gamma_{7,2}$  is given by  $M^2 = \langle \Gamma_{7,2} | J | \Gamma_{7,1} \rangle^2$  ( $\Gamma = +$  or  $-$ ). Considering only the nearest neighbor exchange  $I_1$  [along (1,0,0)] and the next nearest neighbor exchange  $I_2$  [along (1,1,0)], the exchange interaction is

$$I(q) = 2I_1 [\cos(2q_x) + \cos(2q_y) + \cos(2q_z)] \\ + 2I_2 [\cos(2(q_x - q_y)) + \cos(2(q_y - q_z)) + \cos(2(q_z - q_x)) \\ + \cos(2(q_x + q_y)) + \cos(2(q_y + q_z)) + \cos(2(q_z + q_x))]: \quad (3)$$

In a two sub-lattice picture constituted of alternating (1,1,1) planes where the spins are up or down,  $I_1$  would correspond to the antiferromagnetic exchange between spins from different sublattices and  $I_2$  would correspond to the ferromagnetic exchange between spins from the same sublattice. A global fit to the dispersion curves of equation (2) is shown in figure 4. It gives the exchange terms  $M^2 I_1 = 0.354 \pm 0.040$  meV and  $M^2 I_2 = 0.028 \pm 0.013$  meV and the  $\Gamma$  splitting  $\Gamma = 2.812 \pm 0.480$  meV. The corresponding spin-wave gap is  $\Delta = E(0) = 1.28$  meV.

The exchange energy can be expressed by  $E_{\text{ex}} = \frac{2J(J+1)}{3} I(0)$ . Taking the wave functions of  $\Gamma_{7,1}$  and  $\Gamma_{7,2}$  when there is neither exchange nor distortion [17] gives us an approximated square transition matrix element  $M^2 = 2.78$  thus  $I(0) = 0.64 \pm 0.18$  meV. With  $J = 5/2$ , we obtain  $E_{\text{ex}} = 3.71$  meV. The ratio  $E_{\text{CF}} = E_{\text{ex}}/3$  permits then to conclude that the CF energy is of the same order than the exchange interaction

that justifies the treatment of the spin wave using the molecular-field random-phase approximation.

## 4. Discussion

### 4.1. Kondo temperature

We have analyzed the  $Q$ -independent excitations using two contributions, one corresponding to quasielastic scattering and the other to a crystal-field transition. Since these excitations overlap with each other and with the incoherent peak (see figure 2), the energy, width, and weight of the different contributions extracted from the data depend on the model used for the fitting. This is illustrated by the scatter in the estimates of  $\omega_{CF}$ ,  $\omega_{CF}$ , and  $\omega_{QE}$  found in the literature [10, 11, 18, 19]. At low temperatures, the QE excitation corresponds to the spin fluctuations of the  $\gamma$  electronic level, which are attributed to the Kondo effect. Its width ( $\text{HWHM}$ )  $\omega_{QE}$  corresponds to the Kondo temperature. A Kondo temperature of  $T_K = 10$  K at a pressure of  $P = 19$  kbar was obtained in <sup>115</sup>In-NQR measurements by Kawasakiet al. [20]. It is likely that below this pressure the anomaly at  $T_N$  in the  $1/T_1$  temperature variation masks the  $T_K$  anomaly. We assume therefore that  $T_K$  has a very slight variation for pressures below  $P = 19$  kbar, so that it is only slightly smaller than 10 K at ambient pressure. Resistivity measurements give a Kondo scattering maximum at  $T_M \approx 50$  K [4], which corresponds to the high Kondo temperature  $T_K^h = \frac{3}{2} T_K (\omega_{CF} = k_B T)^2$  [21]. INS gives  $\omega_{CF} = 10.6$  meV which with  $T_K^h = 50$  K leads to  $T_K \approx 8$  K. It is then reasonable to approximate the Kondo temperature by  $T_K \approx 10$  K in CeIn<sub>3</sub> at ambient pressure. For the INS measurement carried out at  $T = 5$  K  $< T_K$ , we choose consequently to fix the QE width to  $\omega_{QE} = k_B T_K = 0.86$  meV. The fact that  $\omega_{CF} = 5.7$  meV is relatively large compared to  $\omega_{QE} = 0.86$  meV is due to the larger spin fluctuations associated with the  $\gamma$  first excited level. In fact, the CF transition  $\gamma \rightarrow \delta$  has a width corresponding to the convolution of the  $\gamma$  and  $\delta$  widths  $\omega_{CF}^7 = \omega_{QE}^7$  and  $\omega_{QE}^8$ . We can approximate  $\omega_{CF} \approx \omega_{QE}^7 + \omega_{QE}^8$  and thus estimate that  $\omega_{QE}^8 \approx \omega_{CF} - \omega_{QE}^7 = 4.84$  meV, which is effectively 5 times larger than  $\omega_{QE}$ .

### 4.2. Anisotropy

Even if the CF level is broad, it seems that the propagating spin waves can be described by considering  $\gamma$  as an "isolated" doublet split by the anisotropy and exchange fields. Since this doublet originates from a sixfold degenerate  $J = 5/2$  level, an anisotropy gap is expected in the spin-wave spectrum. We recall that in the isotropic case, the spin-wave dispersion has no gap, since only the exchange is responsible for the splitting

The gap of the spin wave excitation corresponds to its minimum energy that is obtained at  $q = (0;0;0)$ . Since this excitation overlaps with the incoherent elastic scattering that reflects the experimental resolution and with the quasielastic

contribution of the spin fluctuations, the gap was not correctly obtained in the present neutron experiment. The given value of  $\Delta$  corresponds to the best fit to the data using the spin-wave model described above. An attempt to directly observe the gap using a smaller incident energy (and hence better resolution) on the cold triple-axis spectrometer IN 12 (ILL) failed because of the strong indium absorption cross-section. A determination of the energy gap was also made by low-temperature specific-heat measurements which exhibited a spin wave contribution that leads to a gap  $\Delta = 0.69$  meV [22]. This suggests that the gap energy of 1.28 meV deduced from our INS measurements is somewhat overestimated.

The result of our spin-wave analysis is in good agreement with calculations made by Wang et al. for Ce<sup>3+</sup> ions under cubic crystal field and effective exchange field [17]. They consider a molecular field along the c-axis, which can be approximated by  $g_B H_m = k_B T_N$ , and calculate the level splitting as a function of  $g_B H_m = B_4$ . Knowing that for CeIn<sub>3</sub>  $T_N = 10.1$  K,  $\Delta_{CF} = 10.6$  meV and hence  $B_4 = 2.94 \cdot 10^2$  meV ( $\Delta_{CF} = 360 B_4$ ), we have  $g_B H_m = 8.71 \cdot 10^1$  meV  $\approx 30 B_4$ . For this value of  $g_B H_m = B_4$ , Wang et al. calculate a  $\gamma$  splitting of about  $40 B_4 \approx 1.2$  meV. Although we suppose that in our case the molecular field is not along the c-axis (see below), we believe that Wang's calculations give the right order of the splitting.

There are several indications for that the moments are not along the c-axis. If the CF alone imposes the easy magnetization axis, the positive sign of  $B_4$  in the CF Hamiltonian implies that the moments are along the [1,1,1] direction in the ordered phase. This is also supported by nuclear quadrupolar resonance measurements [23]. Although it is difficult to determine the moment direction of a cubic compound by neutron diffraction, some recent measurements also suggest that the moments are not along the c-axis [22].

#### 4.3. Comparison with CePd<sub>2</sub>Si<sub>2</sub>

CeIn<sub>3</sub> seems to have a behavior very similar to the HF compound CePd<sub>2</sub>Si<sub>2</sub> which is antiferromagnetically ordered at ambient pressure and has the same kind of excitation spectrum with coexisting QE, CF, and spin-wave excitations [24]. The characteristic energies are very close and, moreover, unconventional superconductivity appears at a similar external pressure [3]. A summary of the characteristic physical quantities of those two compounds is given in Table 1. A focus on the few differences between those two compounds can be made as following. Firstly CePd<sub>2</sub>Si<sub>2</sub> is tetragonal while CeIn<sub>3</sub> is cubic. Some characteristics such as the CF splitting or the susceptibility anisotropy can be directly linked to anisotropy effects that are resulting from those lattice structures. Then, the characteristic quantities  $T_C$  and  $\Delta$  are twice bigger in CePd<sub>2</sub>Si<sub>2</sub> than in CeIn<sub>3</sub>, that could traduce an enhancement of the spin fluctuations in the tetragonal CePd<sub>2</sub>Si<sub>2</sub>. As a supplement to the studies of quasi 2D  $Ce_m T_n In_{3m+2n}$  compounds where  $T_C$  can reach more than 2 K, an alternative way to study the influence of anisotropy in strongly correlated systems could consequently remain in a detailed comparison between cubic

Table 1. Characteristic physical quantities of CeIn<sub>3</sub> and CePd<sub>2</sub>Si<sub>2</sub>. Data are taken from [3], [4], [22], [24], [25], [26], [27], [28].

	CeIn <sub>3</sub>	CePd <sub>2</sub> Si <sub>2</sub>
T <sub>N</sub>	10.1 K	10 K
k	(1/2,1/2,1/2)	(1/2,1/2,0)
m <sub>0</sub>	0.50 <sub>B</sub>	0.62 <sub>B</sub>
	0.69 meV	0.83 meV
Bandwidth	2 meV	2 meV
P	-50 K	-47 K
T <sub>K</sub>	10 K	10 K
C <sub>F</sub>	123 K	220 and 280 K
P <sub>C</sub>	26.5 kbar	28.6 kbar
T <sub>C</sub>	200 mK	430 mK
	130 mJmol <sup>-1</sup> K <sup>-2</sup>	250 mJmol <sup>-1</sup> K <sup>-2</sup>

: DC susceptibility measurement along a-axis

:  $\chi = C/T$  at low T

CeIn<sub>3</sub> and tetragonal CePd<sub>2</sub>Si<sub>2</sub>.

## 5. Conclusion

We have performed the first inelastic neutron scattering measurements on single crystals of CeIn<sub>3</sub>. The combined use of time-of-flight and triple-axis spectrometers allowed us to study both local and dispersive low-energy excitations. We found the coexistence below T<sub>N</sub> of a spin-wave with a quasielastic component and a crystal-field excitation. The CF levels are substantially broadened by Kondo-type spin fluctuations, which indicates the proximity to an intermediate valence state where the CF collapse. Despite the smearing of the CF levels, the observation of spin waves means that the ground state level in CeIn<sub>3</sub> is also relatively well-defined. The challenge is then to understand how these excitations evolve on going toward a QCP where the hierarchy between the Kondo effect and the RKKY coupling is reversed while the CF should be close to a collapse.

## Acknowledgments

We acknowledge the help of K. Momy for sample preparation and X-ray characterization. We thank also A. P. Murani for many useful and stimulating discussions.

## References

- [1] Morin P., Vettier C., Flouquet J., Konczykowski M., Lassailly Y., Mignot J.M. and Welp U. 1988 *J Low Temp Phys* 70 377.
- [2] Benoit B., Boucherle J.X., Convert P., Flouquet J., Palleau J. and Schweizer J. 1980 *Solid State Comm.* 34 293.
- [3] Mathur N.D., Grosche F.M., Julian S.R., Walker I.R., Freye D.M., Haselwimmer R.K.W. and Lonzarich G.G. 1998 *Nature* 394 39.
- [4] Knebel G., Braithwaite D., Canfield P.C., Lapertot G., Flouquet J. 2001 *Phys. Rev. B* 65 24425.
- [5] Millis A. 1993 *Phys. Rev. B* 48 7183.
- [6] Moriya T. and Takimoto T. 1995 *J. Phys. Soc. Japan* 64 960.
- [7] Thompson J.D., Movshovich R., Fisk Z., Bouquet F., Curro N.J., Fisher R.A., Hammel P.C., Hegger H., Hundley M.F., Jaime M., Pagliuso P.G., Petrovic C., Phillips N.E. and Sarrao J.L. 2001 *J. Magn. Magn. Mat.* 226-230 5.
- [8] Monthoux P. and Lonzarich G.G. 2001 *Phys. Rev. B* 63 054529.
- [9] Petrovic C., Pagliuso P.G., Hundley M.F., Movshovich R., Sarrao J.L., Thompson J.D., Fisk Z., and Monthoux P. 2001 *J. Phys.: Condens. Matter* 13 L337.
- [10] Lawrence J.M. and Shapiro S.M. 1980 *Phys. Rev. B* 22 4379.
- [11] Murani A.P., Taylor A.D., Osborn R. and Bowden Z.A. 1993 *Phys. Rev. B* 48 10606.
- [12] Canfield P.C. and Fisk Z. 1992 *Philos. Mag. B* 65 1117.
- [13] Lea K.R., Leask M.J.M., Wolf W.P. 1962 *J. Phys. Chem. Solids* 23 1381.
- [14] Buschow K.H.J., DeWijn H.W. and Van Diepen A.M. 1969 *J. Chem. Phys.* 50 137.
- [15] Boucherle J.X., Flouquet J., Lassailly Y., Palleau J. and Schweizer J. 1983 *J. Magn. Magn. Mat.* 31-34 409.
- [16] Buyers W.J.L., Holden T.M. and Perreault A. 1975 *Phys. Rev. B* 11 266.
- [17] Wang Y.L. and Cooper B.R. 1970 *Phys. Rev. B* 2 2607.
- [18] Grover W., Knorr K., Murani A.P. and Buschow K.H.J. 1980 *Z. Phys. B* 37 123.
- [19] Lassailly Y., Burke S.K. and Flouquet J. 1985 *J. Phys. C* 18 5737.
- [20] Kawasaki S., Mito T., Zheng G.-Q., Thessieu C., Kawasaki Y., Ishida K., Kitaoka Y., Muramatsu T., Kobayashi T.C., Aoki D., Araki S., Haga Y., Settai R. and Onuki Y. 2001 *Phys. Rev. B* 65 020504.
- [21] Hanzawa K., Yamada K. and Yosida K. 1985 *J. Magn. Magn. Mat.* 47-48 357.
- [22] Knafo W. et al., in preparation
- [23] Kohori Y., Kohara T., Yamato Y., Tomka G. and Riedl P.C. 2000 *Physica B* 281-282 12.
- [24] Van Dijk N.H., Fak B., Charvolin T., Lejay P. and Mignot J.M. 2000 *Phys. Rev. B* 61 8922.
- [25] Grier B.H., Lawrence J.M., Murgai V. and Parks R.D. 1984 *Phys. Rev. B* 29 2664.
- [26] Demuer A., Jaccard D., Sheikin I., Raymond S., Salce B., Thomasson J., Braithwaite D. and Flouquet J. 2001 *J. Phys. Condens. Matter* 13 9335.
- [27] Steeman R.A., Mason T.E., Lin H., Buyers W.J.L., Menovsky A.A., Collins M.F., Frikkee E., Nieuwenhuys G.J. and Mydosh J.A. 1990 *J. Appl. Phys.* 67 5203.
- [28] Grosche F.M., Julian F.R., Mathur N.D. and Lonzarich G.G. 1996 *Physica B* 223-224 50.

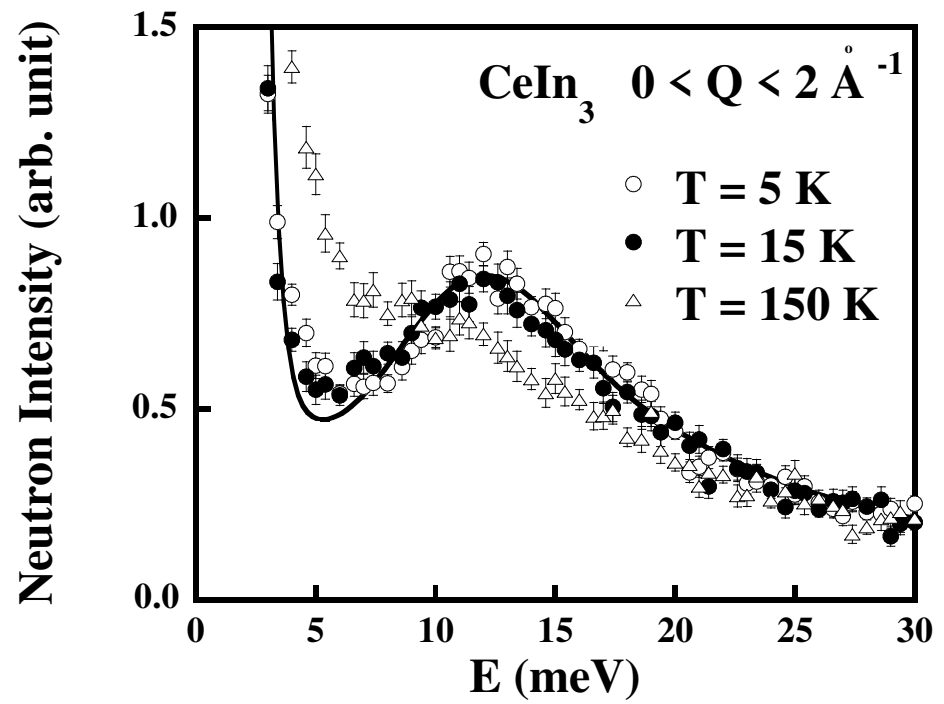


Figure 1. Energy scans at different temperatures obtained on MARI spectrometer using an incident energy of 60.3 meV and integrating over  $Q$  values between 0 and  $2 \text{ \AA}^{-1}$ . The solid line shows the total fit for  $T = 5 \text{ K}$ .

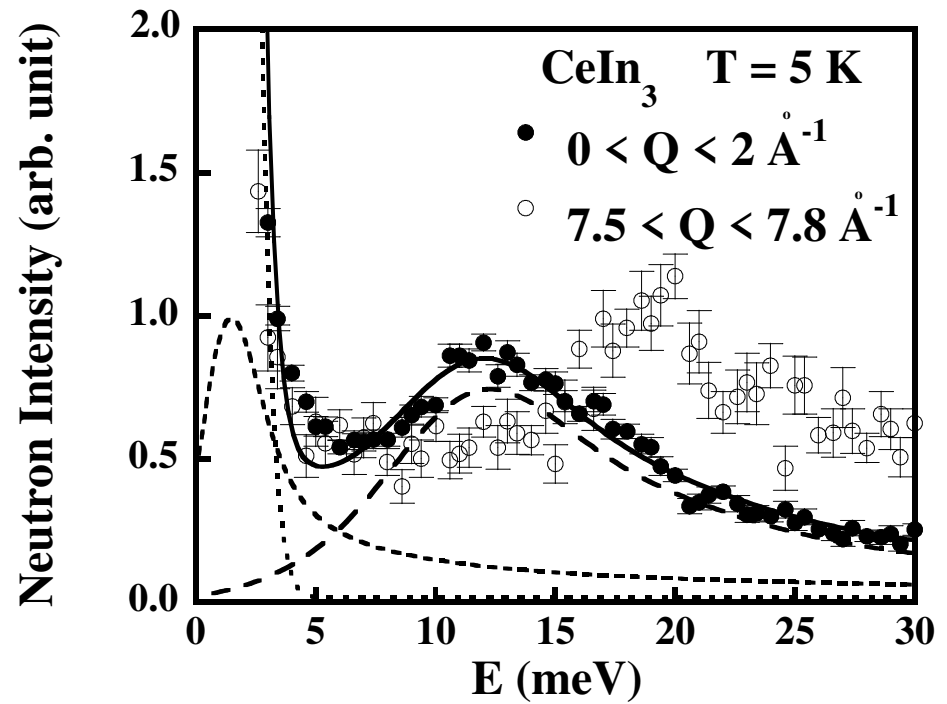


Figure 2. Energy scans at different wavevectors obtained on the MARI spectrometer using an incident energy of 60.3 meV at  $T = 5$  K. The long dashed, short dashed, and dotted lines show the CF, QE, and incoherent contributions of the small  $Q$  spectrum, respectively, while the solid line shows the total.

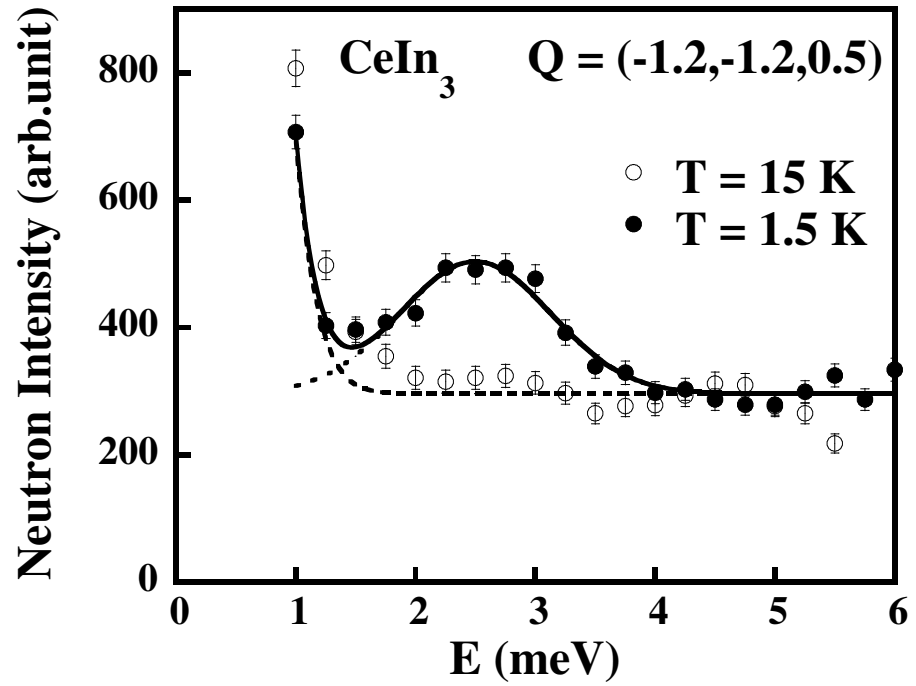


Figure 3. Energy scans at  $Q = (-1.2, -1.2, 0.5)$  for temperatures of  $T = 1.5$  and  $15$  K obtained on the IN22 spectrometer using a final energy of  $14.7$  meV.

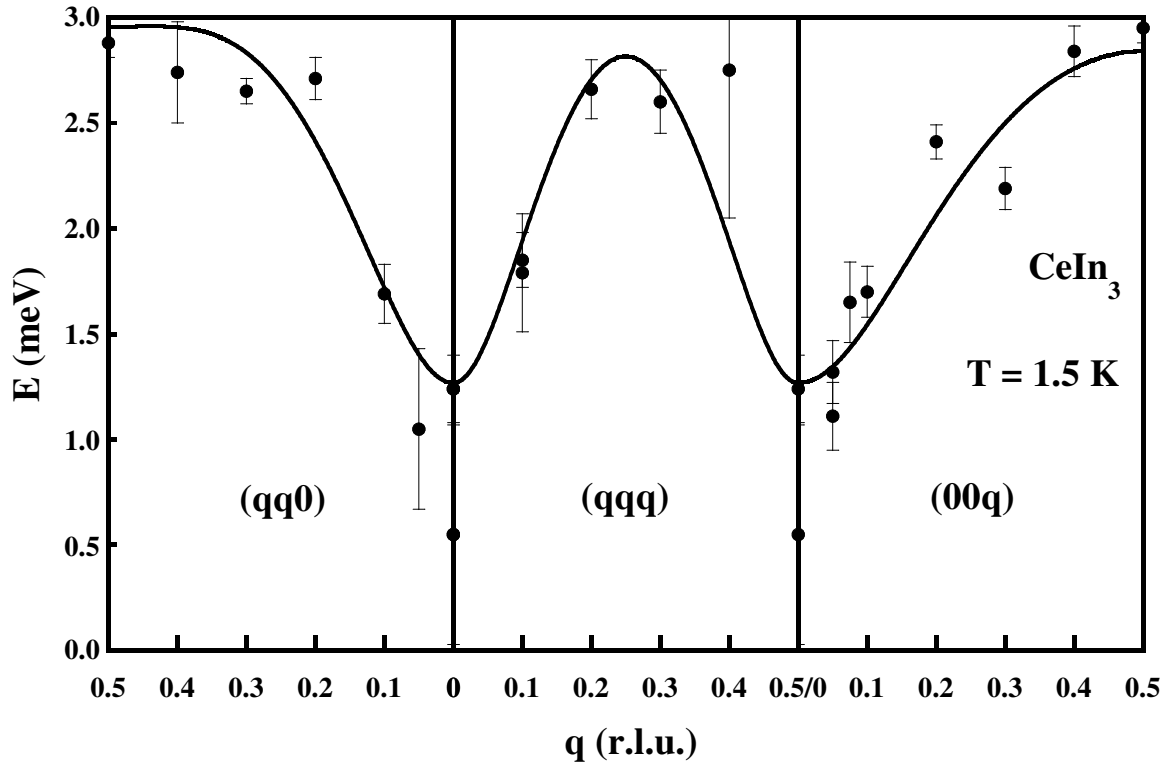


Figure 4. Spin-wave dispersion of  $\text{CeIn}_3$  along the three main directions  $(0;0;q)$ ,  $(q;q;0)$  and  $(q;q;q)$  at  $T = 1.5 \text{ K}$ , obtained on the IN22 spectrometer using a neutron energy of  $14.7 \text{ meV}$ . The solid line is a fit obtained using the molecular-field random-phase approximation.